LU TP 04-18
August 5, 2004

Oligomerization of Amyloid Aβ_{16-22} Peptides Using Hydrogen Bonds and Hydrophobicity Forces

Giorgio Favrin, Anders Irbäck and Sandipan Mohanty*

Complex Systems Division, Department of Theoretical Physics
Lund University, Sölvegatan 14A, SE-223 62 Lund, Sweden
http://www.thep.lu.se/complex/

Submitted to *Biophys. J.*

Abstract:
The 16–22 amino acid fragment of the β-amyloid peptide associated with the Alzheimer's disease, Aβ, is capable of forming amyloid fibrils. Here we study the aggregation mechanism of Aβ_{16-22} peptides by unbiased thermodynamic simulations at the atomic level for systems of one, three and six Aβ_{16-22} peptides. We find that the isolated Aβ_{16-22} peptide is mainly a random coil in the sense that both the α-helix and β-strand contents are low, whereas the three- and six-chain systems form aggregated structures with a high β-sheet content. Furthermore, in agreement with experiments on Aβ_{16-22} fibrils, we find that large parallel β-sheets are unlikely to form. For the six-chain system, the aggregated structures can have many different shapes, but certain particularly stable shapes can be identified.

*E-mail: favrin, anders, sandipan@thep.lu.se

1 Introduction

The fibrillar aggregates that characterize amyloid diseases, such as the Alzheimer's disease, are formed by specific peptides or proteins. However, it is known that several non-disease-related proteins are capable of forming similar amyloid structures [1, 2], and that the aggregation of such proteins can be cytotoxic [3]. This suggests, first, that polypeptide chains have a general tendency to form amyloid structures and, second, that natural proteins should have evolved mechanisms to avoid this tendency. Such mechanisms have indeed been proposed [4–6]. The propensity of a given polypeptide chain to form amyloid fibrils depends, nevertheless, on its amino acid sequence [7–11], and short sequence stretches promoting amyloid formation have been identified [12, 13].

While the structure of amyloid fibrils is not known in atomic detail, there is ample evidence from X-ray fiber diffraction studies that the core of the typical amyloid fibril is composed of β-sheets whose strands run perpendicular to the fibril axis [14]. More detailed information is available, for example, for fibrils made from different fragments of the Alzheimer's Aβ peptide. In particular, there is evidence from solid-state NMR studies for a parallel organization of the β-strands in Aβ_{10-35} [15] and Aβ_{1-40} [16] fibrils, and for an antiparallel organization in Aβ_{34-42} [17], Aβ_{11-25} [18] and Aβ_{16-22} fibrils [19, 20]. Most of these fragments contain the hydrophobic Aβ_{16-20} segment (KLVFF), which is known to be important in the Aβ-Aβ interaction [21].

Small peptides like Aβ_{16-22} are well suited as model systems for probing the mechanisms of aggregation and fibril formation, and are being studied not only *in vitro* but also *in silico*. Computer simulations of simplified [22–26] and atomic [27–31] models have provided useful insights into the aggregation behavior of some peptide systems. To properly explore the free-energy landscape of aggregation at the atomic level is, nevertheless, a computational challenge.

Here we investigate the formation and properties of Aβ_{16-22} oligomers by unbiased Monte Carlo (MC) simulations of systems with up to six chains, using a sequence-based atomic model with an effective potential based on hydrogen bonds and hydrophobic attraction (no explicit water molecules). The same model has previously been used to study the folding of individual peptides [32–34]. It was shown that this model is able to fold several different peptides, both α-helical and β-sheet peptides, for one and the same choice of parameters. The calculated melting behaviors were, moreover, in good agreement with experimental data for all these peptides.

2 Model and Methods

The main object of study in this paper is the peptide Aβ_{16-22}, given by acetyl-Lys-Leu-Val-Phe-Phe-Ala-Glu-NH_2. We consider systems of one, three and six Aβ_{16-22} peptides. The multichain systems are contained in periodic boxes. All the interactions are short range, which makes the implementation of the periodic boundary conditions straightforward. The box sizes are $(35\text{Å})^3$ and $(44\text{Å})^3$ for three and six chains, respectively, corresponding to a constant peptide concentration. For computational efficiency, the peptide concentration is taken to be high.

Our model [32–34] contains all atoms of the peptide chains, including hydrogen atoms. The model assumes fixed bond lengths, bond angles and peptide torsion angles (180°), so that each amino acid only has the Ramachandran torsion angles ϕ, ψ and a number of side-chain torsion angles as its degrees of freedom. Numerical values of the geometrical parameters held constant can be found elsewhere [32].

The interaction potential

$$E = E_{\text{ev}} + E_{\text{loc}} + E_{\text{hb}} + E_{\text{hp}} \tag{1}$$

is composed of four terms, which we describe next. Energy parameters are given on a scale such that a temperature of $T = 300\,\text{K}$ corresponds to $kT \approx 0.447$ (k is Boltzmann's constant) [34].

The first term in Eq. 1, E_{ev}, represents excluded-volume effects and has the form

$$E_{\text{ev}} = \kappa_{\text{ev}} \sum_{i<j} \Big[\frac{\lambda_{ij}(\sigma_i + \sigma_j)}{r_{ij}} \Big]^{12}, \tag{2}$$

where the summation is over pairs of atoms (i, j), $\kappa_{\text{ev}} = 0.10$, and $\sigma_i = 1.77$, 1.75, 1.55, 1.42 and 1.00 Å for S, C, N, O and H atoms, respectively. The parameter λ_{ij} has the value 0.75 for all pairs except those connected by three covalent bonds, for which $\lambda_{ij} = 1$. When the two atoms belong to different chains, we always use $\lambda_{ij} = 0.75$. To speed up the calculations, Eq. 2 is evaluated using a cutoff of $r_{ij}^{\text{c}} = 4.3\lambda_{ij}\,\text{Å}$, and pairs with fixed separation are omitted.

The second energy term, E_{loc}, is a local intrachain potential. It has the form

$$E_{\text{loc}} = \kappa_{\text{loc}} \sum_{I} \left(\sum \frac{q_i q_j}{r_{ij}^{(I)}/\text{Å}} \right), \tag{3}$$

where the inner sum represents the interactions between the partial charges of the backbone NH and C′O groups in one amino acid, I. This potential is not used for Gly and Pro amino acids which have very different ϕ, ψ distributions, but is the same for all other amino acids. The inner sum has four terms (NC′, NO, HC′ and HO) which depend only on the ϕ and ψ angles for amino acid I. The partial charges are taken as $q_i = \pm 0.20$ for H and N and $q_i = \pm 0.42$ for C′ and O [35], and we put $\kappa_{\rm loc} = 100$, corresponding to a dielectric constant of $\epsilon_r \approx 2.5$.

The third term of the energy function is the hydrogen-bond energy $E_{\rm hb}$, which has the form

$$E_{\rm hb} = \epsilon_{\rm hb}^{(1)} \sum_{\rm bb-bb} u(r_{ij}) v(\alpha_{ij}, \beta_{ij}) + \epsilon_{\rm hb}^{(2)} \sum_{\rm sc-bb} u(r_{ij}) v(\alpha_{ij}, \beta_{ij}) \,, \tag{4}$$

where the two functions $u(r)$ and $v(\alpha, \beta)$ are given by

$$u(r) = 5\Big(\frac{\sigma_{\rm hb}}{r}\Big)^{12} - 6\Big(\frac{\sigma_{\rm hb}}{r}\Big)^{10} \tag{5}$$

$$v(\alpha, \beta) = \begin{cases} (\cos\alpha \cos\beta)^{1/2} & \text{if } \alpha, \beta > 90^\circ \\ 0 & \text{otherwise} \end{cases} \tag{6}$$

We consider only hydrogen bonds between NH and CO groups, and r_{ij} denotes the HO distance, α_{ij} the NHO angle and β_{ij} the HOC angle. The parameters $\epsilon_{\rm hb}^{(1)}$, $\epsilon_{\rm hb}^{(2)}$ and $\sigma_{\rm hb}$ are taken as 3.1, 2.0 and 2.0 Å, respectively. The function $u(r)$ is calculated using a cutoff of $r^{\rm c} = 4.5$ Å. The first sum in Eq. 4 contains backbone-backbone interactions, while the second sum contains interactions between charged side chains (Asp, Glu, Lys and Arg) and the backbones. For intrachain hydrogen bonds we make two restrictions. First, we disallow backbone NH (C′O) groups to make hydrogen bonds with the two nearest backbone C′O (NH) groups on each side of them. Second, we forbid hydrogen bonds between the side chain of one amino acid with the nearest donor or acceptor on either side of its C_α. For interchain hydrogen bonds, we make no such restrictions. As a simple form of context dependence, we assign a reduced strength to hydrogen bonds involving chain ends, which tend to be exposed to water. Following the experimental studies of the Aβ_{16-22} peptide [19,20], we have used acetyl and amide capping groups at the ends. A hydrogen bond involving one or two such groups is reduced in strength by factors of 2 and 4, respectively.

The fourth energy term, $E_{\rm hp}$, represents an effective hydrophobic attraction between nonpolar side chains. It has the pair-wise additive form

$$E_{\rm hp} = -\sum_{I<J} M_{IJ} C_{IJ} \,, \tag{7}$$

		I	II	III
I	Ala	0.0	0.1	0.1
II	Ile, Leu, Met, Pro, Val		0.9	2.8
III	Phe, Trp, Tyr			3.2

Table 1: The hydrophobicity matrix M_{IJ}. Hydrophobic amino acids are divided into three categories. The matrix M_{IJ} represents the size of hydrophobicity interaction when an amino acid of type I is in contact with an amino acid of type J.

where C_{IJ} is a measure of the degree of contact between side chains I and J, and M_{IJ} sets the energy that a pair in full contact gets. The matrix M_{IJ} is defined in Table 1. To calculate C_{IJ} we use a predetermined set of atoms, A_I, for each side chain I. We define C_{IJ} as

$$C_{IJ} = \frac{1}{N_I + N_J} \Big[\sum_{i \in A_I} f(\min_{j \in A_J} r_{ij}^2) + \sum_{j \in A_J} f(\min_{i \in A_I} r_{ij}^2) \Big] , \tag{8}$$

where the function $f(x)$ is given by $f(x) = 1$ if $x < A$, $f(x) = 0$ if $x > B$, and $f(x) = (B - x)/(B - A)$ if $A < x < B$ [$A = (3.5\,\text{Å})^2$ and $B = (4.5\,\text{Å})^2$]. Roughly speaking, C_{IJ} is the fraction of atoms in A_I or A_J that are in contact with some atom from the other side chain. For Pro, the set A_I consists of the C_β, C_γ and C_δ atoms. The definition of A_I for the other hydrophobic side chains has been given elsewhere [32]. For pairs that are nearest or next-nearest neighbors along the same chain, we use a reduced strength for the hydrophobic attraction; M_{IJ} is reduced by a factor of 2 for next-nearest neighbors, and taken to be 0 for nearest neighbors.

To study the thermodynamic behavior of this model, we use simulated tempering [36–38] in which the temperature is a dynamical variable. For a review of simulated tempering and other generalized-ensemble techniques for protein folding, see Ref. [39]. We study the one- and three-chain systems at eight different temperatures, ranging from 275 K to 369 K, and the six-chain system at seven temperatures, ranging from 287 K to 369 K.

Our simulations are carried out using two different elementary moves for the backbone degrees of freedom: first, the highly non-local pivot move in which a single backbone torsion angle is turned; and second, a semi-local method [40] that works with up to eight adjacent backbone degrees of freedom, which are turned in a coordinated manner. Side-chain angles are updated one by one. In addition to these updates, we also use rigid-body translations and rotations of whole chains. Every update involves a Metropolis accept/reject step, thus ensuring detailed balance. All our simulations are started from random configurations. All statistical errors quoted are 1σ errors

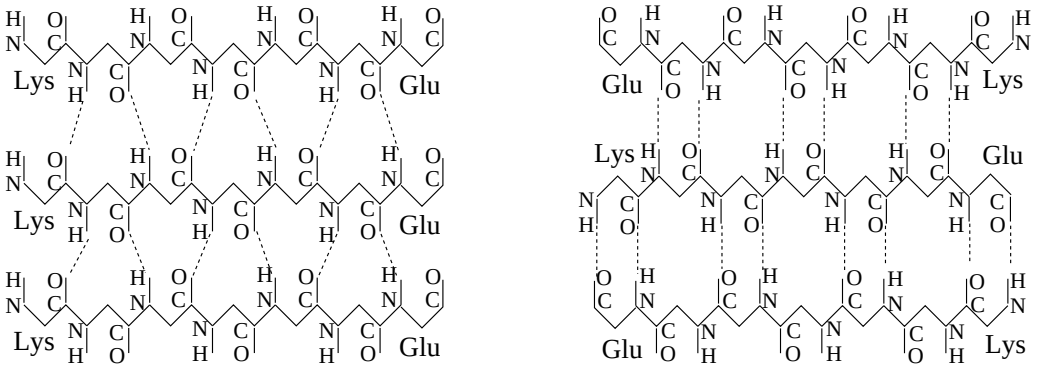

Figure 1: Schematic illustrations of the hydrogen bond patterns for in-register, parallel β-strands (left) and in-register, antiparallel β-strands (right).

obtained from the variation between independent runs. We performed 9 runs with 10^8 elementary MC steps for $N_c = 1$, 11 runs with 10^9 MC steps for $N_c = 3$, and 18 runs with $2 \cdot 10^9$ MC steps for $N_c = 6$. Each of the $N_c = 6$ runs required about 12 CPU days on a 1.6 GHz computer.

To characterize the behavior of these systems, we first determine the secondary structure. For a chain with N amino acids, we define the α-helix and β-strand contents as the fractions of the $N - 2$ inner amino acids with their (ϕ, ψ) pair in the α-helix and β-strand regions of the Ramachandran space. We assume that α-helix corresponds to $-90^\circ < \phi < -30^\circ$, $-77^\circ < \psi < -17^\circ$ and that β-strand corresponds to $-150^\circ < \phi < -90^\circ$, $90^\circ < \psi < 150^\circ$. The average α-helix and β-strand contents, over all the chains of the system, are denoted by H and S, respectively.

To distinguish between parallel and antiparallel β-sheet structure, we examine the orientation of end-to-end vectors. For a given multichain configuration, we first determine all pairs of chains such that (i) their interchain hydrogen bond energy is less than $-1.5\epsilon_{hb}^{(1)}$ (roughly corresponding to 2–3 hydrogen bonds), and (ii) both chains have a β-strand content higher than 0.5. For each such pair of chains, we then calculate the scalar product of their normalized end-to-end unit vectors. If this scalar product is greater than 0.7 (less than -0.7), we say that the two chains are parallel (antiparallel). We denote the numbers of parallel and antiparallel pairs of chains by n_+ and n_-, respectively. Fig. 1 illustrates the hydrogen-bond patterns in parallel and antiparallel β-sheets.

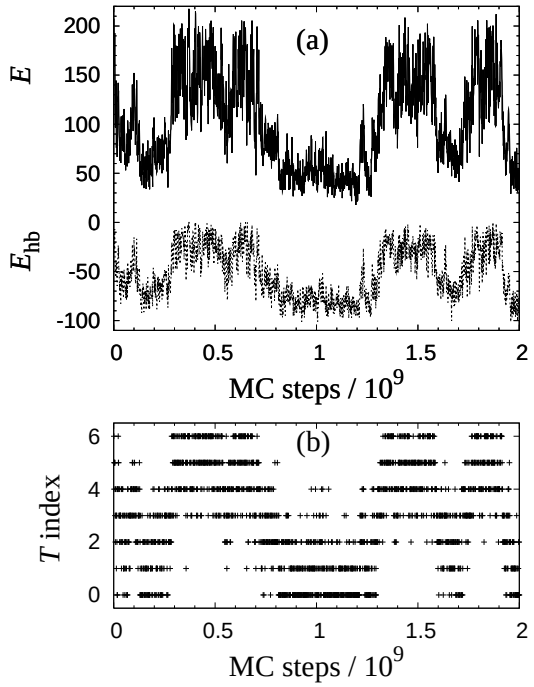

Figure 2: Monte Carlo evolution in a simulated-tempering run for $N_c = 6$ Aβ_{16-22} peptides. (a) The total energy E (full line) and the hydrogen-bond energy E_{hb} (dashed line), both in kcal/mol. (b) The temperature index k. There are seven allowed temperatures T_k, satisfying $T_0 = 287\,\mathrm{K} < T_1 < \ldots < T_6 = 369\,\mathrm{K}$. Measurements are taken every 10^6 MC steps.

3 Results and Discussion

Using the model described in the previous section, we study the thermodynamics of systems of N_c Aβ_{16-22} peptides for $N_c = 1$, 3 and 6. Fig. 2 illustrates the Monte Carlo evolution in one of 18 independent simulated-tempering runs for the six-chain system. In the course of the run, aggregated low-energy structures form and dissolve several times.

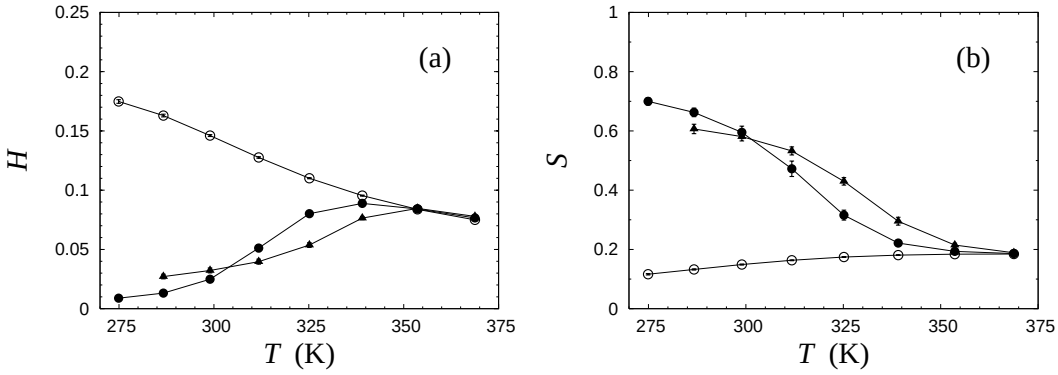

Figure 3: (a) The α-helix content H against temperature T for Aβ_{16-22} for $N_c = 1$ ($\circ$), $N_c = 3$ ($\bullet$) and $N_c = 6$ ($\blacktriangle$). Lines joining data points are only a guide for the eye. (b) Same for the β-strand content S. Note that the scales in (a) and (b) are different.

3.1 Secondary Structure

Fig. 3 shows the α-helix and β-strand contents H and S, as defined in the previous section, against temperature for different N_c. For $N_c = 1$, we see that both H and S are small at all temperatures studied, although H increases with decreasing temperature. So, in our model, the Aβ_{16-22} monomer is mainly a random coil throughout this temperature range. The $N_c = 3$ and $N_c = 6$ systems show a qualitatively different behavior; S increases sharply with decreasing temperature, to values of $S = 0.6$ and higher, whereas H is very small. These results clearly demonstrate that unless the temperature is too high, the three- and six-chain systems self-assemble into ordered structures with a high β-strand content.

The temperature at which the aggregation sets in depends strongly on the peptide concentration, and exploring that dependence is beyond the scope of the present study. We note, however, that the β-sheet formation sets in at a higher temperature for $N_c = 6$ than for $N_c = 3$. This fact is also reflected in the behavior of the specific heat, as shown in Fig. 4. For $N_c = 3$ and $N_c = 6$, the specific heat $C_v(T)$ exhibits a pronounced peak. As the system size increases from $N_c = 3$ to $N_c = 6$, the peak is shifted towards higher temperature. Near the peak, the energy distribution is broad (data not shown), showing that both aggregated low-energy and unstructured high-energy states occur with a significant frequency at these temperatures.

Our results for $N_c = 1$ and $N_c = 3$ can be compared with results from molecular dynamics simulations with explicit water by Klimov and Thirumalai [29]. Using

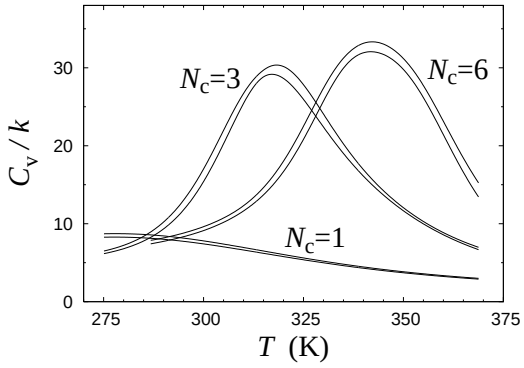

Figure 4: Specific heat C_v against temperature T for $N_c = 1$, 3 and 6 Aβ_{16-22} peptides, as obtained using histogram reweighting techniques [41]. The bands are centered around the expected values and show statistical 1σ errors. C_v is defined as $C_v = (N_c N)^{-1} d\langle E\rangle/dT = (N_c N k T^2)^{-1}(\langle E^2\rangle - \langle E\rangle^2)$, where N_c is the number of chains, N is the number of amino acids per chain, and $\langle O\rangle$ denotes a Boltzmann average of variable O.

somewhat different definitions of H and S and a temperature of $T = 300\,\mathrm{K}$, these authors found that $H = 0.11$ and $S = 0.33$ for $N_c = 1$, and $H = 0.26$ and $S = 0.30$ for $N_c = 3$. Our $N_c = 1$ results (see Fig. 3) are in reasonable agreement with theirs, given that we use a stricter definition and β-strands. However, our $N_c = 3$ results disagree with theirs. They obtained a smaller β-strand content and a larger α-helix content compared to their own $N_c = 1$ results; whereas we observe a much larger β-strand content for $N_c = 3$ compared to $N_c = 1$.

For the $N_c = 3$ system, Klimov and Thirumalai [29] furthermore found evidence for an obligatory α-helical intermediate. To see whether or not such an intermediate exists in our model, we divided the energy axis into bins and calculated the average α-helix and β-strand contents for each bin, at a fixed temperature near the specific heat maximum. Fig. 5 shows the resulting α-helix and β-strand profiles $H(E)$ and $S(E)$. We see that the β-strand content $S(E)$ increases steadily with decreasing energy. The α-helix content $H(E)$, on the other hand, does have its global maximum at $E \sim 130\,\mathrm{kcal/mol}$. However, the maximum value of $H(E)$ is very small. Hence, we find no sign of an obligatory α-helical intermediate in our model. Most of the amino acids in a typical configuration at intermediate energies are either random coils or β-strands.

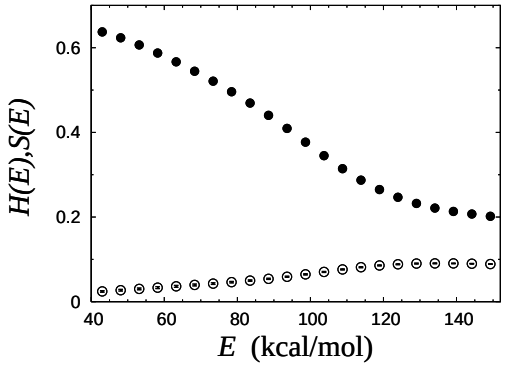

Figure 5: The α-helix ($\circ$) and β-strand ($\bullet$) profiles $H(E)$ and $S(E)$ (see the text) for the six-chain Aβ_{16-22} system at $T = 325\,\mathrm{K}$.

3.2 β-Strand Organization

As mentioned in the introduction, there exist experimental results [19, 20] suggesting that the β-strands in full Aβ_{16-22} fibrils have an in-register, antiparallel organization. To find out whether our systems show a preference for either parallel or antiparallel β-sheets, we consider the joint probability distribution $P(n_+, n_-)$, where n_+ and n_- count the numbers of interacting chain pairs with high β-strand contents that are parallel and antiparallel, respectively (see Sec. 2).

Table 2 shows this distribution for the $N_\mathrm{c} = 3$ system at $T = 275\,\mathrm{K}$. For this system, the most probable combination of (n_+, n_-) is $(1, 1)$, corresponding to a mixed β-sheet. At the same time, the distribution shows a clear asymmetry. The frequency of occurrence for antiparallel β-sheets with $(n_+, n_-) = (0, 2)$ is a factor of 7 higher than that for parallel β-sheets with $(n_+, n_-) = (2, 0)$.

The corresponding results for $N_\mathrm{c} = 6$, at $T = 287\,\mathrm{K}$, are shown in Table 3. As in the $N_\mathrm{c} = 3$ case, we find that a majority of the configurations contain mixed β-sheet structure, n_+ and n_- both being nonzero. The asymmetry of the (n_+, n_-) distribution is even more pronounced for $N_\mathrm{c} = 6$ than for $N_\mathrm{c} = 3$. In particular, we see that large n_- values are much more probable than large n_+ values; the combination $(n_+, n_-) = (4, 0)$ is, e.g., very unlikely to occur, whereas $(n_+, n_-) = (0, 4)$ does occur with a significant frequency.

Tables 2 and 3 show the (n_+, n_-) distribution at the lowest temperatures studied. With increasing temperature, the average n_+ and n_- steadily decrease. At the highest temperature studied, 369 K, about 99% of the conformations have $n_+ = n_- = 0$, for

n_+	n_-		
	0	1	2
0	0.17 (2)	0.22 (3)	0.14 (3)
1	0.13 (2)	0.32 (6)	
2	0.020 (7)		

Table 2: The probability distribution $P(n_+, n_-)$ (see Sec. 2) for $N_c = 3$ Aβ_{16-22} peptides at $T = 275\,\mathrm{K}$. $P(n_+, n_-)$ values smaller than 10^{-3} are omitted. The numbers in parentheses are the statistical errors in the last digits.

n_+	n_-				
	0	1	2	3	4
0	0.028 (5)	0.059 (11)	0.08 (2)	0.06 (2)	0.030 (15)
1	0.038 (6)	0.12 (2)	0.16 (3)	0.10 (3)	0.006 (3)
2	0.026 (11)	0.11 (5)	0.14 (5)	0.004 (2)	
3	0.008 (5)	0.013 (9)	0.015 (12)		

Table 3: Same as Table 2 for $N_c = 6$ Aβ_{16-22} peptides at $T = 287\,\mathrm{K}$.

$N_c = 3$ as well as $N_c = 6$. The full (n_+, n_-) distribution for both $N_c = 3$ and $N_c = 6$ at all the different temperatures studied can be found as Supplementary Material.

Although the statistical uncertainties are somewhat large, the results in Tables 2 and 3 show some clear trends. The most striking one is that large n_+ values are strongly suppressed, which means that large parallel β-sheets are very unlikely to form. The probability of having large antiparallel β-sheets is much higher. Compared to purely antiparallel β-sheet structures, it is possible that mixed β-sheet structures are more difficult to extend to large stable structures. To be able to check whether or not this is the case, simulations of larger systems are required.

Why are antiparallel β-sheets favored over parallel ones? Klimov and Thirumalai [29] concluded that Aβ_{16-22} peptides make antiparallel β-sheets because of Coulomb interactions between charged side chains; the two end side chains of the Aβ_{16-22} peptide carry opposite charges, which indeed should make the antiparallel orientation electrostatically favorable. However, our model completely ignores Coulomb interactions between side-chain charges and still strongly favors the antiparallel organization. Other mechanisms than Coulomb interactions between side-chain charges might therefore play a significant role, such as the geometry of backbone-backbone hydrogen bonds (see Fig. 1), steric effects, and the precise distribution of hydrophobicity along the

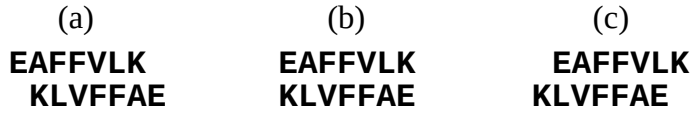

Figure 6: Schematic representations of three different registries for an antiparallel pair of Aβ_{16-22} peptides.

chains. A recent experimental study [20] highlights the importance of the hydrophobicity distribution. This study showed that the β-sheet structure of Aβ_{16-22} fibrils can be changed from antiparallel to parallel by adding an octanyl end group to the peptide which increases its amphiphilicity.

To probe the registry of the β-sheets, we monitored backbone-backbone hydrogen bond patterns (see Fig. 1). Fig. 6 illustrates three possible antiparallel registries: (a) $17 + k \leftrightarrow 20 - k$, (b) $17 + k \leftrightarrow 21 - k$, and (c) $17 + k \leftrightarrow 22 - k$. The $17 + k \leftrightarrow 21 - k$ registry is the one found in experiments on Aβ_{16-22} fibrils [19, 20], whereas experiments on fibrils made from the slightly larger segment Aβ_{11-25} found evidence for the $17 + k \leftrightarrow 20 - k$ registry at pH 7.4 and for the $17 + k \leftrightarrow 22 - k$ registry at pH 2.4 [18]. In our calculations, the $17 + k \leftrightarrow 20 - k$ and $17 + k \leftrightarrow 21 - k$ registries occur with high and comparable frequencies. The $17 + k \leftrightarrow 22 - k$ registry is, by contrast, strongly suppressed, which probably is due to hydrophobic effects, although steric clashes between the large Phe side chains could play a role, too. As to the $17 + k \leftrightarrow 20 - k$ and $17 + k \leftrightarrow 21 - k$ registries, it would be very interesting to see whether their relative frequencies of occurrence depend on (n_+, n_-), but that will require higher statistics than those provided by the present calculations.

3.3 Other Peptides

To test our model, we performed simulations similar to those for the Aβ_{16-22} peptide for some other peptides. Some of these peptides, including the polar one studied by Diaz-Avalos *et al.* [42], had a low overall hydrophobicity. We found that the propensity to aggregate is much lower for such peptides than for the Aβ_{16-22} peptide, and a higher peptide concentration was required to promote aggregation. These results clearly show that in our model, hydrophobic attraction is a major driving force for aggregation.

As an example of a peptide with a significant hydrophobicity but an uneven distribution of it, we studied the peptide acetyl-Lys-Phe-Phe-Ala-Ala-Ala-Glu-NH_2, in which the two strongly hydrophobic Phe amino acids are asymmetrically placed. For

this peptide, we obtained aggregated β-sheet structures with a predominantly parallel β-strand organization, which in particular confirms that our model is capable of generating stable parallel β-sheets.

3.4 Examples of Low-Energy Structures

It is known that relatively small assemblies formed early in the aggregation of full-length Aβ [43–45] as well as non-disease-related proteins [3] can be toxic, which makes it very interesting to study possible oligomer shapes. In addition, such structures represent potential seeds for the fibril formation.

From our simulations, we find that the six-chain Aβ_{16-22} system does not exhibit a single dominating free-energy minimum, but rather a number of more or less degenerate local minima. Fig. 7 shows two snapshots of such minima. The β-strand content is, as noted earlier, high, and the structures shown in Fig. 7 illustrate this property.

In the simplest class of typical structures observed in our simulations, five of the chains form a relatively flat β-sheet, whereas the remaining chain is a random coil and held in contact with the β-sheet by hydrophobic attraction. Six-stranded β-sheets also occur in the simulations, but with a low frequency, as can be seen from the $P(n_+, n_-)$ distribution in Table 3. Further, for the six-chain system, we observe the emergence of new non-trivial structures with no analogs in the three-chain simulations. The second structure in Fig. 7 illustrates this. Here stability is achieved by stacking two different, three-stranded, β-sheets together, which brings hydrophobic side chains from the two β-sheets in close contact. Such "sandwiches" occur with a non-negligible frequency in our simulations. To estimate the precise populations of these minima is difficult. However, five-stranded β-sheets did occur more frequently than sandwiches in the simulations. By visual inspection, we further estimate that of the order of 10 % of the configurations are sandwich-like at the lowest temperature studied, at which the snapshots were taken. These low-energy structures also occur at higher temperatures, but become very rare above the specific heat maximum (see Fig. 4).

In none of our simulations did we find any indication of a free-energy minimum in which the β-strands are joined end-to-end to form the so-called β-helix [47]. In our model, stability is enhanced by increasing the number of hydrogen bonds or by increasing hydrophobic contacts. For system sizes as small as those we examined, the β-helix is inferior to many competing structures in both these respects, and hence its absence is expected.

Figure 7: Two typical low-energy structures from our simulations of six Aβ_{16-22} peptides: a five-stranded β-sheet (left), and two three-stranded β-sheets "sandwiching" several of their hydrophobic side-chains between them (right). Drawn with RasMol [46].

4 Conclusion

Using a sequence-based atomic model which was originally developed for folding studies of single peptides [32–34], we studied the aggregation properties of Aβ_{16-22} peptides. In this model, we found that Aβ_{16-22} peptides have a high propensity to self-assemble into aggregated structures with a high β-strand content, while the isolated Aβ_{16-22} peptide is mainly a random coil. Both parallel and antiparallel arrangements of the β-strands occur in the model, with a definite preference for the antiparallel arrangement.

It is important to note that we find this preference for the antiparallel β-strand orientation despite ignoring the Coulomb interactions between the two charged side chains at the ends of the peptide. It has been suggested [29] that such Coulomb interactions are the main determinant for the antiparallel orientation. While these Coulomb interactions might enhance the tendency for Aβ_{16-22} peptides to form β-sheets with an antiparallel organization, our results strongly suggest that other factors play a significant role, too. It is worth noting that the orientation is not necessarily determined solely by sequence-specific side-chain interactions, as antiparallel β-sheets are widely held to be intrinsically more stable than parallel ones. For the Aβ_{16-22} peptide, which in particular lacks a clear amphiphility, there is no obvious mechanism to overcome this tendency.

In our simulations, we did not observe an absolute free-energy minimum, but rather several nearly degenerate minima corresponding to different supra-molecular structures, all consisting of arrangements of β-strands. Apart from single β-sheets, laminated multi-sheet structures were found near free-energy minima for the six-chain

system. It should be pointed out that the six-chain system is still too small to permit the formation of, for example, a barrel-type structure. It will therefore be very interesting to try to extend these calculations to larger system sizes.

Acknowledgments

This work was in part supported by the Swedish Research Council and the Knut and Alice Wallenberg Foundation through the Swegene consortium.

References

[1] Rochet, J.C., and P.T. Lansbury Jr. 2000. Amyloid fibrillogenesis: themes and variations. *Curr. Opin. Struct. Biol.* 10: 60–68.

[2] Dobson, C.M. 2003. Protein folding and misfolding. *Nature* 426: 884–890.

[3] Bucciantini, M., E. Giannoni, F. Chiti, F. Baroni, L. Formigli, J. Zurdo, N. Taddei, G. Ramponi, C.M. Dobson, and M. Stefani. 2002. Inherent toxicity of aggregates implies a common mechanism for protein misfolding diseases. *Nature* 416: 507–511.

[4] Otzen, D.E., O. Kristensen, and M. Oliveberg. 2000. Designed protein tetramer zipped together with a hydrophobic Alzheimer homology: A structural clue to amyloid assembly. *Proc. Natl. Acad. Sci. USA* 97: 9907–9912.

[5] Broome, B.M., and M.H. Hecht. 2000. Nature disfavors sequences of alternating polar and non-polar amino acids: Implications for amyloidogenesis. *J. Mol. Biol.* 296: 961–968.

[6] Richardson, J.S., and D.C. Richardson. 2002. Natural β-sheet proteins use negative design to avoid edge-to-edge aggregation. *Proc. Natl. Acad. Sci. USA* 99: 2754–2759.

[7] West, M.W., W.X. Wang, J. Patterson, J.D. Mancias, J.R. Beasley, and M.H. Hecht. 1999. *De novo* amyloid proteins from designed combinatorial libraries. *Proc. Natl. Acad. Sci. USA* 96: 11211–11216.

[8] Villegas, V., J. Zurdo, V.V. Filimonov, F.X. Avilés, C.M. Dobson, and L. Serrano. 2000. Protein engineering as a strategy to avoid formation of amyloid fibrils. *Protein Sci.* 9: 1700-1708.

[9] Hammarström, P., X. Jiang, A.R. Hurshman, E.T. Powers, and J.W. Kelly. 2002. Sequence-dependent denaturation energetics: a major determinant in amyloid disease diversity. *Proc. Natl. Acad. Sci. USA* 99: 16427–16432.

[10] López de la Paz, M., K. Goldie, J. Zurdo, E. Lacroix, C.M. Dobson, A. Hoenger, and L. Serrano. 2002. *De novo* designed peptide-based amyloid fibrils. *Proc. Natl. Acad. Sci. USA* 99: 16052–16057.

[11] Chiti, F., M. Stefani, N. Taddei, G. Ramponi, and C.M. Dobson. 2003. Rationalization of the effects of mutations on peptide and protein aggregation rates. *Nature* 424: 805–808.

[12] López de la Paz, M., and L. Serrano. 2004. Sequence determinants of amyloid formation. *Proc. Natl. Acad. Sci. USA* 101: 87–92.

[13] Ventura, S., J. Zurdo, S. Narayanan, M. Parreño, R. Mangues, B. Reif, F. Chiti, E. Giannoni, C.M. Dobson, F.X. Aviles, and L. Serrano. 2004. Short amino acid stretches can mediate amyloid formation in globular proteins: the Src homology 3 (SH3) case. *Proc. Natl. Acad. Sci. USA* 101: 7258–7263.

[14] Sunde, M., and C. Blake. 1997. The structure of amyloid fibrils by electron microscopy and X-ray diffraction. *Adv. Protein Chem.* 50: 123–159.

[15] Burkoth, T.S., T.L.S. Benzinger, V. Urban, D.M. Morgan, D.M. Gregory, P. Thiyagarajan, R.E. Botto, S.C. Meredith, and D.G. Lynn. 2000. Structure of the β-amyloid$_{(10-35)}$ fibril. *J. Am. Chem. Soc.* 122: 7883–7889.

[16] Petkova, A.T., Y. Ishii, J.J. Balbach, O.N. Antzutkin, R.D. Leapman, F. Delaglio, and R. Tycko. 2002. A structural model for Alzheimer's β-amyloid fibrils based on experimental constraints from solid state NMR. *Proc. Natl. Acad. Sci. USA* 99: 16742–16747.

[17] Lansbury, P.T., P.R. Costa, J.M. Griffiths, E.J. Simon, M. Auger, K.J. Halverson, D.A. Kocisko, Z.S. Hendsch, T.T. Ashburn, R.G.S. Spencer, B. Tidor, and R.G. Griffin. 1995. Structural model for the β-amyloid fibril based on interstrand alignment of an antiparallel-sheet comprising a C-terminal peptide. *Nat. Struct. Biol.* 2: 990–998.

[18] Petkova, A.T., G. Buntkowsky, F. Dyda, R.D. Leapman, W.M. Yau, and R. Tycko. 2004. Solid state NMR reveals a pH-dependent antiparallel β-sheet registry in fibrils formed by a β-amyloid peptide. *J. Mol. Biol.* 335: 247–260.

[19] Balbach, J.J., Y. Ishii, O.N. Antzutkin, R.D. Leapman, N.W. Rizzo, F. Dyda, J. Reed, and R. Tycko. 2000. Amyloid fibril formation by Aβ_{16-22}, a seven-residue fragment of the Alzheimer's β-amyloid peptide, and structural characterization by solid state NMR. *Biochemistry* 39: 13748–13759.

[20] Gordon, D.J., J.J. Balbach, R. Tycko, and S.C. Meredith. 2004. Increasing the amphiphilicity of an amyloidogenic peptide changes the β-sheet structure in the fibrils from antiparallel to parallel. *Biophys. J.* 86: 428–434.

[21] Tjernberg, L.O., J. Näslund, F. Lindqvist, J. Johansson, A.R. Karlström, J. Thyberg, L. Terenius, and C. Nordstedt. 1996. Arrest of β-amyloid fibril formation by a pentapeptide ligand. *J. Biol. Chem.* 271: 8545–8548.

[22] Bratko, D., and H.W. Blanch. 2001. Competition between protein folding and aggregation: a three-dimensional lattice-model simulation. *J. Chem. Phys.* 114: 561–569.

[23] Harrison, P.M., H.S. Chan, S.B. Prusiner, and F.E. Cohen. 2001. Conformational propagation with prion-like characteristics in a simple model for protein folding. *Protein Sci.* 10: 819–835.

[24] Dima, R.I., and D. Thirumalai. 2002. Exploring protein aggregation and self-propagation using lattice models: phase diagram and kinetics. *Protein Sci.* 11: 1036–1049.

[25] Jang, H., C.K. Hall, and Y. Zhou. 2004. Assembly and kinetic folding pathways of a tetrameric β-sheet complex: Molecular dynamics simulations on simplified off-lattice protein models. *Biophys. J.* 86: 31–49.

[26] Friedel, M., and J.E. Shea. 2004. Self-assembly of peptides into a β-barrel motif. *J. Chem. Phys.* 120: 5809–5823.

[27] Ma, B., and R. Nussinov. 2002. Stabilities and conformations of Alzheimer's β-amyloid peptide oligomers (Aβ_{16-22}, Aβ_{16-35}, and Aβ_{10-35}): sequence effects. *Proc. Natl. Acad. Sci. USA* 99: 14126–14131.

[28] Ma B., and R. Nussinov. 2002. Molecular dynamics simulations of alanine rich β-sheet oligomers: insight into amyloid formation. *Protein Sci.* 11: 2335–2350.

[29] Klimov, D.K., and D. Thirumalai. 2003. Dissecting the assembly of Aβ_{16-22} amyloid peptides into antiparallel β sheets. *Structure* 11: 295–307.

[30] Gsponer, J., U. Haberthür, and A. Caflisch. 2003. The role of side-chain interactions in the early steps of aggregation: Molecular dynamics simulations of an amyloid-forming peptide from the yeast prion Sup35. *Proc. Natl. Acad. Sci. USA* 100: 5154–5159.

[31] Paci, E., J. Gsponer, X. Salvatella, and M. Vendruscolo. 2004. Molecular dynamics studies of the process of amyloid aggregation of peptide fragments of transthyrin. In press: *J. Mol. Biol.*

[32] Irbäck, A., B. Samuelsson, F. Sjunnesson, and S. Wallin. 2003. Thermodynamics of α- and β-structure formation in proteins. *Biophys. J.* 85: 1466–1473.

[33] Irbäck, A., and F. Sjunnesson. 2004. Folding thermodynamics of three β-sheet peptides: a model study. *Proteins* 56: 110–116.

[34] Irbäck, A., and S. Mohanty. 2004. Preprint LU TP 04-28. Submitted to *Biophys. J.*

[35] Brändén, C., and J. Tooze. 1991. *Introduction to Protein Structure*. Garland Publishing, New York.

[36] Lyubartsev, A.P., A.A. Martsinovski, S.V. Shevkunov, and P.N. Vorontsov-Velyaminov. 1992. New approach to Monte Carlo calculation of the free energy: method of expanded ensembles, *J. Chem. Phys.* 96: 1776–1783.

[37] Marinari, E., and G. Parisi. 1992. Simulated tempering: A new Monte Carlo scheme, *Europhys. Lett.* 19: 451–458.

[38] Irbäck, A., and F. Potthast. 1995. Studies of an off-lattice model for protein folding: sequence dependence and improved sampling at finite temperature, *J. Chem. Phys.* 103: 10298–10305.

[39] Hansmann, U.H.E., and Y. Okamoto. 1999. New Monte Carlo algorithms for protein folding. *Curr. Opin. Struct. Biol.* 9: 177–183.

[40] Favrin, G., A. Irbäck, and F. Sjunnesson. 2001. Monte Carlo update for chain molecules: biased Gaussian steps in torsional space. *J. Chem. Phys.* 114: 8154–8158.

[41] Ferrenberg, A.M., and R.H. Swendsen. 1988. New Monte Carlo technique for studying phase transitions. *Phys. Rev. Lett.* 61: 2635–2638.

[42] Diaz-Avalos, R., C. Long, E. Fontano, M. Balbirnie, R. Grothe, D. Eisenberg, and D.L.D. Caspar. 2003. Cross-beta order and diversity in nanocrystals of an amyloid-forming peptide. *J. Mol. Biol.* 330: 1165–1175.

[43] Lambert, M.P., A.K. Barlow, B.A. Chromy, C. Edwards, R. Freed, M. Liosatos, T.E. Morgan, I. Rozovsky, B. Trommer, K.L. Viola, P. Wals, C. Zhang, C.E. Finch, G.A. Krafft, and W.L. Klein. 1998. Diffusive, nonfibrillar ligands derived from Aβ_{1-42} are potent nervous system neurotoxins. *Proc. Natl. Acad. Sci. USA* 95: 6448–6453.

[44] Walsh, D.M., D.M. Hartley, Y. Kusumoto, Y. Fezoui, M.M. Condron, A. Lomakin, G.B. Benedek, D.J. Selkoe, and D.B. Teplow. 1999. Amyloid β-protein fibrillogenesis — structure and biological activity of protofibrillar intermediates. *J. Biol. Chem.* 274: 25945–25952.

[45] Walsh, D.M., I. Klyubin, J.V. Fadeeva, W.K. Cullen, R. Anwyl, M.S. Wolfe, M.J. Rowan, and D.J. Selkoe. 2002. Naturally secreted oligomers of amyloid β protein potently inhibit hippocampal long-term potentiation *in vivo*. *Nature* 416: 535–539.

[46] Sayle, R., and E.J. Milner-White. 1995. RasMol: biomolecular graphics for all. *Trends Biochem. Sci.* 20: 374–376.

[47] Wetzel, R. 2002. Ideas of order for amyloid fibril structure. *Structure* 10: 1031–1036.